

Compact and Highly Efficient 2.5 MHz SiC Electronic Ballast for Inductively Coupled UV Lamps

Christoph Simon¹, Santiago Eizaguirre¹, Fabian Denk², Rainer Kling¹

¹Karlsruhe Institute of Technology, Germany

²Ushio Deutschland GmbH, Germany

Corresponding author: Christoph Simon, christoph.simon@kit.edu

Abstract

Inductively coupled UV lamps require a high-frequency alternating current for ignition and efficient operation. In this work, we present a switch-mode half-bridge inverter, with SiC-MOSFETs, which achieves a conversion efficiency from the DC-Link to a 2.5 MHz alternating current of 95 % at 750 W lamp power, including auxiliary power for the gate drivers and the controller. Furthermore, the paper describes an algorithm for the active power measurement of a 2.5 MHz voltage and current signal with an oscilloscope, averaging in the frequency domain and spectral distinction of the active power at the switching frequency.

1 Introduction

The introduction of power MOSFETs with the wide-bandgap materials silicon carbide (SiC) or gallium nitride (GaN) enables switch-mode inverters with very high switching frequency in the range of 2.5 MHz. Silicon power semiconductors (MOSFETs or IGBTs) switch too slow and overheat from switching losses in that frequency range. Nevertheless, a switching frequency of 2.5 MHz allows a compact design and promises efficiency gains. However, it also increases the stress on passive components and causes a considerable filter effort for electromagnetic compatibility [1] [2].

In the inductively coupled UV lamp, a magnetic field couples the energy into the plasma, which in turn generates the UV radiation. The lamp does not have electrodes and may achieve a longer lifetime because electrode degradation is the primary failure mechanism for lamps with electrodes.

For ignition and operation, the inductively coupled UV lamp requires a high magnetic field time derivative. A system design may increase the derivative with large coils or magnetic cores to increase the magnetic field amplitude but at the cost of more material and losses. Alternatively, the design may increase the frequency of the alternating current source to increase the derivative [3] [4].

A switch-mode inverter with an output frequency of 2.5 MHz and high efficiency is the base for the inductively coupled UV lamp to compete with the conventional lamp with electrodes. The electronic ballast for the conventional lamp with electrodes achieves an efficiency of about 96 % [5]. The high-frequency inverter for inductively coupled lamps needs to achieve that efficiency level as well for the inductively coupled lamp to be useful.

The largest application for UV lamps is disinfection with UV radiation. The UV radiation in the UVC range inactivates most microorganisms so that they cannot reproduce and are no more pathogen. The method does not require any chemicals and leaves no residue behind. Because of this advantage, the market for UV disinfection equipment is significant and grows fast. A recent study [6] estimates a market volume of USD 2.9 billion and predicts a CAGR (Compound Annual Growth Rate) of 12.3 % from 2020 to 2025 for UV disinfection equipment.

2 Inverter

The inverter of the electronic ballast is a resonant half- or full-bridge with zero-voltage switching (ZVS) [7]. While SiC-MOSFETs are capable of fast switching, each switching event still produces a specific loss. Without a reduction of that loss, the power at 2.5 MHz overloads the devices.

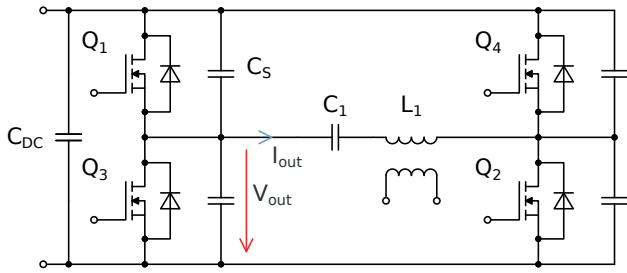


Fig. 1: Schematic of the 2.5 MHz inverter in full-bridge configuration; in a half-bridge, Q_2 and Q_4 are missing, and the second terminal of L_1 is connected to DC-Link ground directly.

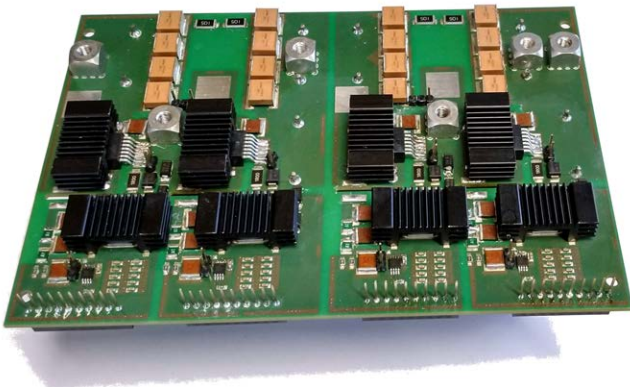


Fig. 2: Image of the 2.5 MHz full-bridge inverter; the two bridge legs are on the left and the right. At the bottom are four connectors for the gate signals and gate driver auxiliary power supply.

Figure 1 shows the schematic of the full-bridge with resonant ZVS and Fig. 2 an image of the inverter PCB. When a MOSFET switches off, the output capacitance of the MOSFET and the snubber capacitors C_s of a bridge leg take over the load current and cause the voltage at the switch node to commute. After the commutation is complete, the other MOSFET can switch on under zero-voltage conditions (ZVS) without losses. The load current is required to be inductive for this by itself or by a resonant circuit. The UV lamp in this application is an inductive load with a low power factor ($\lambda \approx 0.2$ to 0.3) and provides the inductive phase angle for ZVS. Figure 3 shows an image of the lamp.

The layout of the bridge legs is carefully designed for a low-inductance commutation loop so that the snubber capacitors can quickly take over the load current, and noise from the switch node remains at an acceptable level. The SiC-MOSFETs are Cree C3M0065090J in the D2PAK, and the snubber

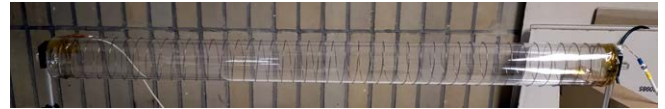


Fig. 3: Image of the inductively coupled UV lamp; a coil is wound around the lamp vessel. In the magnetic field of the coil, a plasma ignites and generates UV radiation.



Fig. 4: Image of the gate driver power supply; each MOSFET has one, and it supplies galvanically isolated -4 V to switch off and 15 V to switch on.

capacitors are CDE Cornell Dubilier MC mica capacitors. Also, the DC-Link needs to sustain the voltage ripple from the switch node, so the DC-Link capacitance is realized with ceramic capacitors TDK CeraLink B58031-series and Vishay MKP1848C DC-Link film capacitors.

2.1 Gate Driver

For a switching frequency of 2.5 MHz, the inverter requires a gate driver with high peak current capability and a carefully designed gate loop for low inductance and fast switching. The gate driver ICs are IXYS IXDN614YI with 14 A peak current. Because of ZVS with an inductive load, the MOSFETs switch on without voltage but switch off at maximum current. The switch-on gate current is limited with a gate resistor in the range from 1Ω to 10Ω to reduce stress on the gate. The switch-off gate current is maximized with an antiparallel diode for minimal resistance during gate discharge. To not overshoot too much, the gate loop has minimal length and low inductance. The endurance of the SiC-MOSFET's gate limits the gate driver's speed. With the 30 A variant of the gate driver, the SiC-MOSFETs tend to fail early.

2.2 Half-Bridge Inverter

A second revision of the inverter is a half-bridge; other than that, it has the same layout and devices. The gate loop is shorter and better optimized towards fast switching. The half-bridge has no

external snubber capacitors and relies only on the output capacitance of the MOSFETs and the capacitances of the PCB for soft-switching. The slew rate of the output voltage at full lamp power of 750 W is about 15 V ns^{-1} . With an external snubber capacitor, the load current is not sufficient to achieve ZVS.

2.3 Controller

The controller of the inverter is a software on a Texas Instruments Piccolo microcontroller; the previous paper [3] presents it in detail.

The microcontroller board is a Texas Instruments Launchpad LAUNCHXL-F280049C with a TMS-320F280049C Piccolo microcontroller. An adapter board connects the Launchpad to the inverter board with LVDS for signal transmission. It provides two channels per MOSFET, one forth for the gate signal and one back for a fault signal from the gate driver. However, the current inverters do not use the fault signals.

Close to the Launchpad pins, the adapter board transforms the single-ended signals of the Launchpad to LVDS with the Texas Instruments LVDS converter DS90LV027 and DS90LV028. Close to the pins of the inverter board, the Analog Devices 5 kV RMS Dual-Channel LVDS Gigabit Isolators ADN4655 transmit the signals through the isolation barrier. On the inverter board, the Texas Instruments LVDS converter DS90LV019 transforms the LVDS signal to single-ended for the gate driver.

Both signal paths of the low-side and the high-side gate driver have the same design, the same isolator device, and the same layout. The symmetric design realizes no runtime differences of the signals. Also, the additional isolator on the low-side increases the decoupling of the controller circuit from the noise of the switch node. The decoupling and LVDS transmission allow the controller to work in proximity to the inverter, connected directly through the adapter board.

3 Active Power Measurement

A voltage and a current measurement of the high-frequency signals at the interface between inverter and load form the base for calculating the active

power, the efficiency, and characterization of the inverter. For this electronic ballast for an inductively coupled UV lamp, the active power at the coil terminals of the lamp is load regarding the efficiency of the inverter. Therefore, the conduction losses of the lamp coil are allocated to the lamp and reduce the UV generation efficiency of the lamp.

The calculation of the active power requires both voltage and current waveforms as well as the phase angle because the exact value of the complex lamp impedance at the coil terminals is unknown and varies over time with lamp heat up and mercury release from the amalgam.

Additionally, because the signals may have significant harmonics, the measurement takes the spectral distribution of the power into account and disregards the active power of the harmonics. The confidence of the active power of a higher harmonic is lower because the accuracy of the amplitudes and the phase angle at a higher frequency generally decreases, mainly because of slight differences in the frequency response of two probes. Disregarding the active power of harmonics reduces distortion of the measurement, and effectively counts that active power as a loss. So an efficiency value based on this measurement underestimates the efficiency slightly but does not overestimate it.

Typical power meters are not well suited for the active power measurement of a 2.5 MHz signal, because their bandwidth is too small. They offer 1 MHz or 10 MHz bandwidth, but even then, the harmonics might be outside the safe-operating-area. Also, the signals usually pass through the device, and it introduces significant additional capacitance and inductance into the resonant circuit.

Thermal or diode power measurement heads for high frequencies are also not well suited because they measure the total power, not a spectral distribution. If connected to the resonant circuit with a directional coupler, they overestimate the active power because the directional coupler has less attenuation at higher frequencies and amplifies the harmonics relative to the signal at the base frequency.

For the characterization of this inverter, a Keysight DSOS104A oscilloscope measures and digitizes the voltage and current waveforms. The voltage

probe is a PMK BumbleBee differential voltage probe and the current probe a Bergoz 0.1 VA⁻¹ current transformer. A program takes the measured waveforms and transforms the time domain signals to the frequency domain with the Fast Fourier Transformation and a flat-top window. Subsequently, it calculates the apparent power, phase angle, and active power of the principal peak in the spectrum. The flat-top window has a small scalloping error, so the amplitude values of the peaks in the frequency domain are valid.

Additionally, for these measurements, the program averages over 30 or 60 spectra in the frequency domain, according to Welch's method [8]. The oscilloscope captures one long waveform in the time domain, and the program splits the waveform into segments with a 50% overlap. It then calculates the Fast Fourier Transformation with a flat-top window of each one, and the arithmetic means of these spectra. The measurement errors caused by the harmonic distortion and noise of the input signals are mostly removed, because of the transformation to the frequency domain and subsequently averaging over several thousand periods in the time domain.

The correct measurement of the active power and the power factor still requires careful deskewing of the voltage and current probes. While the lamp is off, the load impedance is the inductance of an air coil and the copper resistance of the wire, both known from measurement and model. For deskewing, the input voltage is set to a value just before the ignition of the lamp, and the skew value is adjusted so that the power measurement shows the expected phase angle of the coil impedance.

The listings show the Python program for calculating the power values in the frequency domain from the time domain measurements. It requires Python and SciPy—a package for scientific calculations in Python. The program in Lst. 1 first transforms each segment with the Fast Fourier Transformation and a flat-top window and calculates the arithmetic mean of the spectra. Then, the program in Lst. 2 calculates the apparent power, phase angle, and active power from the voltage spectrum and current spectrum.

```
import numpy as np
from numpy.fft import rfft
from scipy.signal.windows import flattop
```

```
N = 2**16
window = flattop(N, sym=False)
```

```
spectrum = np.ndarray(
    (N // 2 + 1, ),
    dtype=np.complex128)
```

```
for i in range(number`of`segments):
    segment = waveform.array[
        i * N // 2 # 50% overlap
        :i * N // 2 + N]
    spectrum += rfft(segment * window)
```

```
spectrum = (spectrum
    # FFT normalization
    / (N / 2)
    # window normalization
    * N / np.sum(window)
    # root mean square
    / np.sqrt(2)
    # averaging
    / number`of`segments)
```

```
# index of the highest peak value
peak = np.argmax(np.abs(spectrum))
```

Lst. 1: Python program for spectrum calculation and averaging

```
import numpy as np
```

```
apparent = (
    np.abs(voltage`spectrum[peak])
    * np.abs(current`spectrum[peak]))
phase = (
    np.angle(voltage`spectrum[peak])
    - np.angle(current`spectrum[peak]))
active`power = apparent * np.cos(phase)
```

Lst. 2: Python program for active power calculation

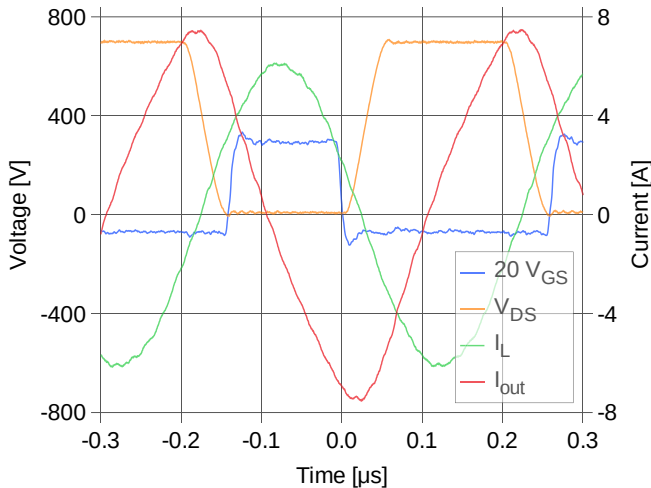


Fig. 5: Switching waveform of the full-bridge inverter at 2.5 MHz and about 750 W lamp power. V_{GS} and V_{DS} of a low-side SiC-MOSFET, I_L and I_{out} . V_{GS} is multiplied by 20.

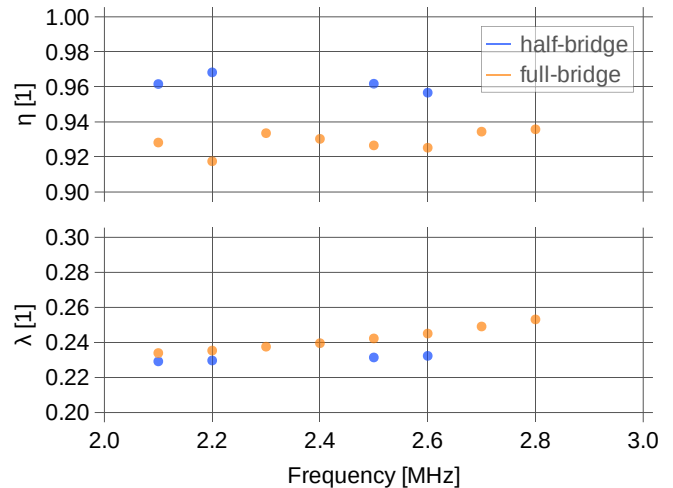


Fig. 6: Efficiency η of the inverter—without auxiliary power—and power factor λ of the lamp over the switching frequency for the half-bridge inverter (blue dots) and the full-bridge inverter (orange dots); the lamp power is 750 W or 700 W respectively.

4 Characterization

The full-bridge and the half-bridge inverter ignite and operate the inductively coupled UV lamp successfully at 2.5 MHz and about 750 W lamp power. Figure 5 shows the switching waveforms of the full-bridge inverter. The SiC-MOSFETs operate under ZVS conditions—the gate voltage V_{GS} only rises after the drain-source voltage V_{DS} reaches zero. The MOSFETs switch off at the maximum output current I_{out} . The output current charges and discharges the output capacitances of the MOSFETs and the snubber capacitors and commutates the voltage.

4.1 Efficiency

Figure 6 shows the efficiency of the power path from the DC-Link to the lamp coil over the frequency from 2.1 MHz to 2.8 MHz at constant active lamp power of 700 W for the full-bridge inverter and 750 W for the half-bridge. The efficiency is about 93 % (orange dots) over the frequency range for the full-bridge inverter and about 96 % (blue dots) for the half-bridge. At the jumps between 2.2 MHz and 2.3 MHz and between 2.6 MHz and 2.7 MHz, the duty cycle was reduced to keep ZVS.

The half-bridge inverter consumes 8.8 W auxiliary power for the gate drivers and controller. The total efficiency is 95 % to supply an inductively coupled UV lamp from a DC-Link with 750 W at 2.5 MHz.

4.2 DC Impedance

By tuning the series capacitor, and keeping the same apparent and active power in the lamp coil, the inverter may show different impedance values at the DC-Link input—in this case from 960 Ω to 390 Ω . Figure 7 shows the efficiency and the DC-Link voltage over the current. The efficiency changes for different operating points, but no clear trend is visible.

However, during the experiment, the SiC-MOSFETs were with about 80 °C considerably hotter for low current and high voltage, than with about 60 °C for high current and low voltage. The temperature difference suggests that the conduction losses in the MOSFETs at about 1 A are not dominant. However, the switching losses due to the voltage swing at each switching event are dominant.

The external snubber capacitors parallel to the MOSFETs take over the commutation current and switching losses from the MOSFET. They could help against high switching losses. However, they also increase the total output capacitance of the inverter and reduce the slew rate, so the inverter requires a higher current to achieve ZVS. But this inverter already barely achieves ZVS at high voltages. For high voltage operation, it would require more power for the load, or a lower power factor.

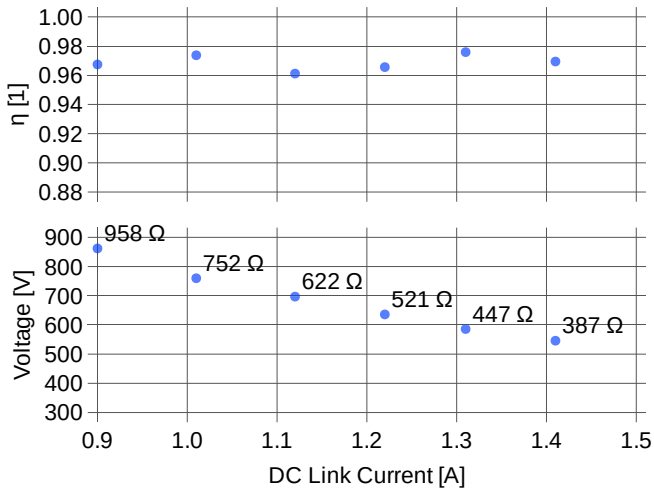


Fig. 7: Efficiency η —without auxiliary power—and DC-Link voltage over current for the half-bridge inverter at 750 W lamp power and 2.2 MHz; a design may select a DC impedance from a broad range without decreasing the efficiency.

4.3 Auxiliary Power Supply

The auxiliary power supply provides 5 V and 3.3 V to the microcontroller and isolated -4 V, 15 V, and logic 5 V (relative to the -4 V) to each gate driver. While the high-side MOSFET requires an isolated gate driver power supply, the low-side MOSFET does not. However, for symmetry and the same behavior of the gate driver and signal transmission, the half-bridge and the full-bridge have the same schematic and layout for the high-side and low-side gate driver and power supply. Additionally, the isolation of the low-side gate driver reduces noise from the switch node in the control circuit.

Both inverters have a modular design and a custom isolated gate driver power supply for each MOSFET. Figure 4 shows an image, and the previous paper [3] presents the module in detail.

For the half-bridge inverter, the microcontroller, the power supply, and signal transmission to the isolation barrier require 1.1 W, which is 0.15% loss at 750 W lamp power. Both gate drivers require together 9.5 W, which is 1.3% loss. In total, the auxiliary power is 10.6 W or 1.4% loss.

For another measurement, we swapped our custom isolated gate driver power supply for Murata Power Solutions MGJ6 Gate Drive DC-DC Converters, MGJ6D121505WMC. With those, the total auxiliary power is 13.9 W or 1.9% for the half-bridge inverter.

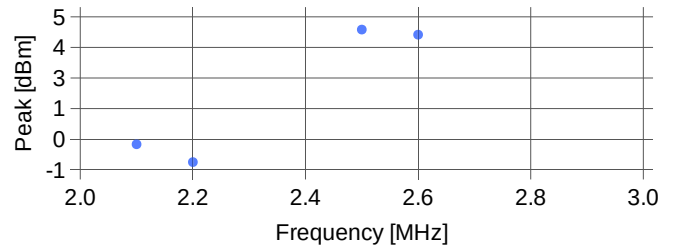


Fig. 8: The first peak's amplitude apart from the base frequency (5th harmonic) over the switching frequency for the half-bridge inverter at 750 W lamp power; at 2.2 MHz, the lamp shows smaller harmonics than at 2.5 MHz.

4.4 Harmonics

The lamp current and voltage show significant harmonics. Depending on the switching frequency, the inverter may excite these minima of the lamp impedance spectrum more or less. Figure 8 shows the amplitude of the first peak apart from the base frequency, which has five times the switching frequency in the range from 10.5 MHz to 13 MHz. At a switching frequency of 2.2 MHz, the harmonics are considerably smaller than at the nominal frequency of 2.5 MHz. At this frequency, the efficiency measurement is also maximal, according to Fig. 6. The lamp power is 750 W for each measurement.

5 Conclusion

The inductively coupled UV lamp may be more efficient and may achieve a longer lifetime than a conventional UV lamp because of no electrode degradation if the electronic ballast provides a high-frequency alternating current with sufficient efficiency. In this work, we present a switch-mode half-bridge inverter that generates a 2.5 MHz alternating current for the lamp with an efficiency of 95% from the DC-Link to the lamp coil terminals at 750 W lamp power, including auxiliary power for the gate driver and controller. The inverter comprises SiC-MOSFETs, a carefully designed switch node for very low inductance, and a powerful gate driver for fast switching. The half-bridge inverter does not have additional snubber capacitors. With this efficiency, the electronic ballast enables the inductively coupled UV lamp to compete in the fast-growing market for UV disinfection equipment and to introduce its advantages in lifetime and efficiency.

References

- [1] J. Biela, M. Schweizer, S. Waffler, and J. W. Kolar, "SiC versus Si—Evaluation of Potentials for Performance Improvement of Inverter and DC–DC Converter Systems by SiC Power Semiconductors", *IEEE Transactions on Industrial Electronics*, vol. 58, no. 7, pp. 2872–2882, 2011. DOI: 10.1109/TIE.2010.2072896.
- [2] C. Simon, F. Denk, M. Heidinger, R. Kling, and W. Heering, "EMI Considerations on MHz Inverters", in *PCIM Europe 2017; International Exhibition and Conference for Power Electronics, Intelligent Motion, Renewable Energy and Energy Management*, May 2017, pp. 1–8.
- [3] C. Simon, S. Eizaguirre, F. Denk, M. Heidinger, R. Kling, and W. Heering, "Control of a SiC 2.5 MHz resonant full-bridge inverter for inductively driven plasma", in *PCIM Europe 2019; International Exhibition and Conference for Power Electronics, Intelligent Motion, Renewable Energy and Energy Management*, May 2019, pp. 1–8.
- [4] O. A. Popov, "Efficient light source based on an inductive ferrite-free discharge at frequencies of 300–3000 kHz", *Technical Physics*, vol. 52, no. 6, pp. 751–758, Jun. 1, 2007. DOI: 10.1134/S1063784207060126.
- [5] eta plus. (Mar. 2, 2020). Elektronische Vorschaltgeräte, [Online]. Available: <https://www.eta-uv.de/de/produkte/elektronische-vorschaltgeraete> (visited on 03/02/2020).
- [6] MarketsandMarkets. (Mar. 2, 2020). UV Disinfection Market by Component & Application - Global Forecast 2023, [Online]. Available: <https://www.marketsandmarkets.com/Market-Reports/uv-disinfection-market-217291665.html> (visited on 03/02/2020).
- [7] M. K. Kazimierczuk and D. Czarkowski, *Resonant power converters*, 2. ed. Hoboken, NJ: Wiley, 2011.
- [8] P. Welch, "The use of fast Fourier transform for the estimation of power spectra: A method based on time averaging over short, modified periodograms", *IEEE Transactions on Audio and Electroacoustics*, vol. 15, no. 2, pp. 70–73, Jun. 1967. DOI: 10.1109/TAU.1967.1161901.

Repository KITopen

Dies ist ein Postprint/begutachtetes Manuskript.

Empfohlene Zitierung:

Simon, C.; Eizaguirre, S.; Denk, F.; Kling, R.

[Compact and Highly Efficient 2.5 MHz SiC Electronic Ballast for Inductively Coupled UV Lamps](#)

2020. International Exhibition and Conference for Power Electronics, Intelligent Motion, Renewable Energy and Energy Management (PCIM Europe digital days 2020), Online, July 7-8, 2020, 1656–1662, VDE Verlag

[doi:10.5445/IR/1000144777](https://doi.org/10.5445/IR/1000144777)

Zitierung der Originalveröffentlichung:

Simon, C.; Eizaguirre, S.; Denk, F.; Kling, R.

[Compact and Highly Efficient 2.5 MHz SiC Electronic Ballast for Inductively Coupled UV Lamps](#)

2020. International Exhibition and Conference for Power Electronics, Intelligent Motion, Renewable Energy and Energy Management (PCIM Europe digital days 2020), Online, July 7-8, 2020, 1656–1662, VDE Verlag

Lizenzinformationen: [KITopen-Lizenz](#)